Modelling Industrial Drives for Power Electronics Studies Part II - Induction Motor

Antonio Carlos S. de Lima and Alquindar Pedroso
COPPE/UFRJ
Universidade Federal do Rio de Janeiro
Programa de Engenharia Elétrica
C.P.68504, Rio de Janeiro
21945-970 RJ Brazil
siqueira@coe.ufrj.br

Abstract— **This work deals with the representation of electric machines for power electronics drives. The main objective is the modelling of induction machines in open loop configurations such as Adjustable Speed Drive. The relevance of an accurate representation of the rotor circuits is of paramount importance to accurately assess the electrogmanetic torque developed by the motor.**

The concept of operational impedance is used to show how the conventional single cage model cannot represent systems with a high harmonic content. Experimental results of a drive system used in the oil exploitation are used to validate the model. Despite the peculiar characteristics of the induction motor used in oil pumping, the model is general enough to represent different types of induction motors.

I. Introduction

The development of electrical drives with power electronic devices has allowed several applications for induction machines. Although very detailed converter controller have appeared in the last two decades, very little has been done regarding the machine modelling. Furthermore, a more precise model produces better results that can even increase the controller response.

The harmonics produced by the inverter excite different currents in the machine rotor. Each one of this harmonics current will contribute to oscillations in the electromagnetic torque. Therefore if a more detailed rotor representation is used one can achieve more information concerning the motor.

The machine modelling is not a new subject, the first works dealing with it date from early 1940's. Those papers discussed steady state calculations or simplified structures for dynamic simulations. During the late 1960's and 1970's, the modelling of induction motors received small attention. The inclusion of semiconductor power switches in the late 1970's made possible reliable variable frequency drive systems. This brought up a new interest in the modelling of induction motors.

In a power electronic drive system there is a steady-state full of harmonics. The harmonics produce hazardous effects such as increase in the motor temperature, torque oscillations, decrease in the overall performance and efficiency. Conventional steady-state based models cannot infer precisely the motor behaviour. It is then very important to evaluate the motor impedance correctly so the stator currents and the electromagnetic torque are represented accordingly. The MicroTran program has recently implemented a new routine for induction machines [1]. It shares the synchronous machine code, extenting it to be used for induction motors. This new routine also allows for a coupling between rotors circuits that eases the implementation of a detailed model. In this paper it is shown how this coupling can affect the simulation results.

II. Induction Machine Equations

The behaviour of the machine is described by two sets of equations, the voltage and the flux linkage.

In matrix notation the voltage equations becomes,

$$\mathbf{v} = \mathbf{R} \cdot \mathbf{i} + \frac{\mathbf{d}}{\mathbf{dt}} \mathbf{\Lambda} \tag{1}$$

and the flux equation is given by,

$$\mathbf{\Lambda} = \mathbf{L} \cdot \mathbf{i} \tag{2}$$

where

$\mathbf{R}$ is a diagonal matrix of winding resistance
$\mathbf{i}$ is the current vector $[i_a, i_b, i_c, i_{d_1}, i_{q_1}, \ldots]$
$\mathbf{v}$ is input voltage vector $[v_a, v_b, v_c, 0, \ldots]$
$\mathbf{L}$ is the inductance matrix given by

$$\mathbf{L} = \begin{bmatrix} L_{11} & L_{12} & \cdots & L_{1n} \\ \vdots & \vdots & \vdots & \vdots \\ L_{n1} & \cdots & \cdots & L_{nn} \end{bmatrix} \tag{3}$$

The solution of (1) is complicated because the elements of the inductance matrix (3) are function of the rotor position, therefore they are function of time t. Park's transformation is used to solve the equation in the $dq0$ domain. The main advantage of this transformation is to have time-independent inductances, decoupling the system in 3 independent equations.

The Park's transformation implemented corresponds to a transformation to two orthogonal rotating axes at rotor speed. The relations are

$$\mathbf{\Lambda}_{dq0} = \mathbf{T}^{-1}\mathbf{\Lambda}_{abc}$$

where

$$\mathbf{T}^{-1} = \begin{bmatrix} \mathbf{T}_1^{-1} & \mathbf{0} \\ \mathbf{0}^{\mathbf{T}} & \mathbf{1} \end{bmatrix} \tag{4}$$

$\mathbf{0}$ is a zero 4×3 matrix, $\mathbf{1}$ is a 4×4 identity matrix, and

$$\mathbf{T}_1^{-1} = \begin{bmatrix} \frac{\sqrt{2}}{\sqrt{3}}\cos\theta & \frac{\sqrt{2}}{\sqrt{3}}\cos(\theta-120^0) & \frac{\sqrt{2}}{\sqrt{3}}\cos(\theta-120^0) \\ \frac{\sqrt{2}}{\sqrt{3}}\sin\theta & \frac{\sqrt{2}}{\sqrt{3}}\sin(\theta-120^0) & \frac{\sqrt{2}}{\sqrt{3}}\cos(\theta-120^0) \\ \frac{1}{\sqrt{3}} & \frac{1}{\sqrt{3}} & \frac{1}{\sqrt{3}} \end{bmatrix} \tag{5}$$

The induction machines have commonly cylindrical rotors. So the air gap is uniform, i.e., both d and q axis have the same parameters. It is also assumed:

- sinusoidal winding distribution, three stator winding electrically spaced by 120^0;
- spatial harmonics are considered to have a minimal effect so as they can be disregarded;
- saturation effects are not considered;
- the maximum number of rotors circuit per axis is two.

The reason for limiting the number of rotor circuits was rather practical, usually one does not have enough information concerning the machine to use more rotor circuits. The double-circuit for the rotor aims the representation of the cage effects over an extended frequency range.

This set of equations creates a system with 7 variables, 3 for the stator, 2 for the d-axis rotor and 2 for the q-axis rotor. If necessary, additional rotor circuits can be added with minimal code change.

The flux-current relationships can be divided in three sets, one for the direct axis, one for the quadrature axis and one equation for the zero sequence. Keeping in mind that there is no saliency, the equation for the quadrature axis is analogous to the direct axis one.

$$\begin{bmatrix} \lambda_d \\ \lambda_{d_1} \\ \lambda_{d_2} \end{bmatrix} = \begin{bmatrix} L_d & L_{dd_1} & L_{dd_2} \\ L_{dd_1} & L_{d_1} & L_{d_1d_2} \\ L_{dd_2} & L_{d_1d_2} & L_{d_2} \end{bmatrix} \cdot \begin{bmatrix} i_d \\ i_{d_1} \\ i_{d_2} \end{bmatrix} \tag{6}$$

and the electromagnetic torque will be

$$\tau = \lambda_d \cdot i_q - \lambda_q \cdot i_d. \tag{7}$$

There are some points worth to comment here, it was not assumed that all mutual are equal in (6). Therefore it is possible to represent the additional coupling between rotor circuits. Whether an identical mutual was considered, only one mutual flux would link all windings on one axis, and the leakage flux of any winding would be linked only with that winding itself. This assumption leads to the classical star circuit representation.

Unlikely the synchronous machine where there are cases where the mechanical part can be ignored, e.g., simulation of short-circuit for just a few cycles, the mechanical part must be represented in induction motors. The mechanical system is considered linear, which is usually correct for the studies here involved. A single mass representation is usually adequate for small motors or large motors with linear load, or motors without long rotors mass. Although there are situations where single-mass system cannot be used, e.g., very large motors or a motor with long rotor. In these cases a number of lumped mass should be used. The matrix equation (8) describes the behaviour of the mechanical system.

$$\begin{cases} \mathbf{J}\dfrac{d^2}{dt^2}\mathbf{\Theta} + \mathbf{D}\dfrac{d}{dt}\mathbf{\Theta} + \mathbf{K}\mathbf{\Theta} = T_{elec} - T_{mech} \\ \dfrac{d}{dt}\mathbf{\Theta} = \mathbf{\Omega} \end{cases} \tag{8}$$

where $\mathbf{J}$ is a diagonal matrix of the the moment of inertia of the rotating mass (motor and mechanical load), $\mathbf{\Theta}$ and $\mathbf{\Omega}$ are vectors of angular positions and speed respectively. $\mathbf{D}$ is a tridiagonal matrix of damping coefficients, $\mathbf{K}$ is a tridiagonal matrix of damping associated with the linear displacement. T_{elec} - T_{mech} is the vector of the net torque injected in the mechanical system.

A. Equivalent Circuit for the Induction Machine

Assuming that each inductance can be expressed as a sum of leakage and mutual inductance one can develop the circuit shown in Fig. 1. The inductance L_0 represents the coupling between rotor circuits and R_1, L_1 are the resistance and inductance for the first cage and R_2, L_2 are the resistance and inductance for the second one. Since the induction motor is symmetrical, the d and q circuits are basically identical. The q-axis circuit differs from the d-axis one only in the sign of the speed voltage. It was assumed also that two cages would be enough to represent the rotor circuits.

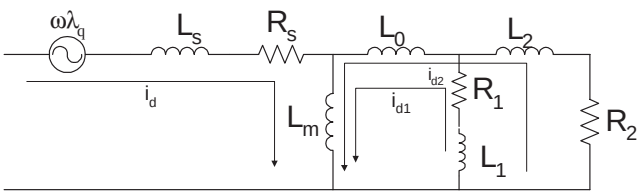

Fig. 1. Equivalent circuit for the induction machine

As the harmonic order increases, the harmonic slip will tend to unity [2]. Since the harmonics will be presented in the high torque region is necessary if not mandatory to use a model capable of representing the motor behaviour at this situation. It can be shown that the coupling between rotor cage is rather important if accuracy at high slip is intended.The square wave inverter can be understood as

a worst case scenario where harmonics produced by the inverter are of order:

$$h = 6k \pm 1$$

where h is the harmonic order, and $h = 1, 2, 3, \ldots$. The $6k+1$ harmonics generate a positive sequence rotating field, and the $6k-1$ produce a negative sequence field. The motor slip is given by

$$s_h = 1 \pm \frac{\omega_r}{h\omega_s} \tag{9}$$

where ω_r, ω_s are the motor and synchronous speed respectively.

The sign in (9) changes with the harmonics. Positive sequence harmonics will have a slip less than 1 (they have a negative sign in (9). Naturally, negative sequence harmonics will have higher than 1 slip. For instance, for a motor speed about 0.95pu, the fifth and the seventh harmonic slip are approximately 1.19 and 0.81 respectively.

The inductance L_0 provides a additional coupling for the rotor circuits. It means that the magnetic coupling between the rotor circuits is stronger than the coupling among the rotor circuit and the main magnetic path. In the case of synchronous machine this inductance is commonly known as Canay Reactance [3]. The value of L_0 affects directly the current distribution in the cages and therefore the torque developed by the motor.

Single cage models can be used when the variation in rotor resistance and inductance is assumed to be negligible. The use of a single cage model implies that the rotor resistance and inductance are defined for only one frequency, and uniform current distribution in the rotor bars is consequently assumed. This results in large errors in the torque developed at low speeds (high slip) for squirrel cage rotors with bars more than 12mm in depth [4]. To illustrate the effect of the frequency in the rotor bars let's assume a simple case with a rectangular rotor bar as seen in Fig. 2(a). Assuming the permeability of iron to be infinite, an analytical expression for the current density $J(y, f)$ can be derived [5]:

$$J(y, f) = \frac{\cosh y\tau}{\tau \sinh \tau d} \tag{10}$$

where

$$\tau = -\frac{1+j}{\delta}$$

and $\delta = \sqrt{\frac{1}{\pi f \mu \sigma}}$, and d is the height of the rotor slot. Fig. 2(b) shows how the frequency affects the current density along the bar. Each frequency creates a different current distribution in the bar, as the frequency goes higher the distribution of the current density becomes considerably non-uniform. In actual rotors however, one cannot find such simple geometries as in Fig. 2(a). To represent actual rotors bars one commonly divide the rotor bar so each part can be represented approximately by a simple rotor bar with a constant current density. If needed, transmission line models can be used to calculate the equivalent rotor bar. Jordan [6] applied this technique to determine the bar current distribution of an induction motor at stall and full load. Levy et al. [7] provided a detailed examination of lumped parameter approach. Honsinger [8] used an equivalent circuit with parallel branches when operating with an inverter. De Donker [9] proposed the use of a double-cage rotor model to provide deep bar compensation in drives with field-oriented control. Healey [10] presented a model with double-cage and saturation effect. It was then used in a vector controlled VSI-PWM inverter.

(a) rectangular bar

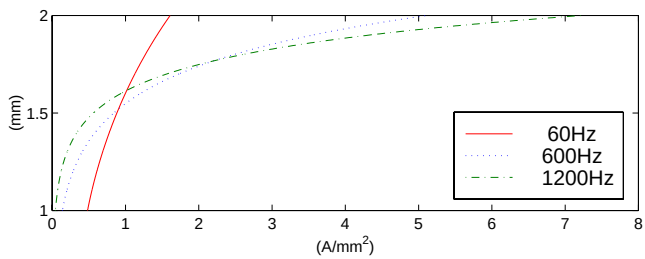

(b) dependence with the rotor depth and frequency

Fig. 2. Current density in rotor bar

All these results stress that a better model can improve the knowledge of the motor behaviour. Nonetheless, all those methodologies require knowledge of the rotor bar geometry. Usually one has only nameplate information, detailed description of the rotor bar design is not commonly available. It is also difficult to determine the most suitable lumped parameter circuit and the minimum number of bar sections required. Rogers and Shirmohammadi in [11] developed an algorithm to build a double-cage model for EMTP programs. It used basically nameplate data and some considerations for the startup of the motor, such as startup current. The problem with this procedure lies in the fact that there are situations where the algorithm fails to converge and only a single-cage model is obtained [12] [13]. Motors with a high rotor resistance are an example of such situation. The algorithm has also a minor drawback, in the first iterations, the values of the stator and the magnetizing inductance are very low. An interactive solution is used then to "boost" this values nearer the actual ones. This results in values for the stator and magnetizing inductance lower than the real ones.

In this work, a method based on the work of Rogers is used to derive the motors parameters. Manufacturers

usually have only single-cage parameters which are only useful when steady-state with sinusoidal voltage or current. However, it provide useful information about stator and magnetizing impedance. This values are then used as input for the algorithm. Unlike the work of Rogers, here the inductance of the first cage is not is taken into account. The algorithm has then to calculate only 5 variables, namely, linkage between rotor circuits, resistance and inductance of the two cages.

III. ESP Motor

Nowadays, the only option for down-hole installation is to use induction motors. Those induction motors are specially designed to work in a pipe and have mineral oil as insulation medium. They are commonly referred as Electrical Submersible Pump (ESP) Motor. They are designed to withstand the high temperature of crude oil flow passing outside of the motor. The maximum temperature rises are limited to 140^0C [14]. On one hand, the motor diameter is quite low, around 15-20cm. On the other hand these motor is considerably long, 2–10m. Depending on the power level of the installation, the set pump motor can reach more than 20m. The stator windings are continuous coils, the rotors are made of small sections that stack for higher horsepower, and the motors has only two poles. One particular characteristic of thi type of motor is the low inertia. If compared with conventional motor of the same voltage and power range, the inertia of the ESP is around one tenth. This stress even further the importance of a detailed motor model. The low inertia makes the motor more susceptible to shaft failure due to harmonic torque. Table III shows the basic characteristics of the ESP motors. The upper limit of 540HP and 400A are only for motors at 440V designed to work in fresh water. For well oil motors the limits are 400HP, and 100A respectively.

TABLE I
Basic Characteristics of ESP motors

Voltage level (V)	440–6000
Current level (A)	50–400
Power output (HP)	100–600
Power Factor	0.81–0.85
Efficiency	0.85–0.91

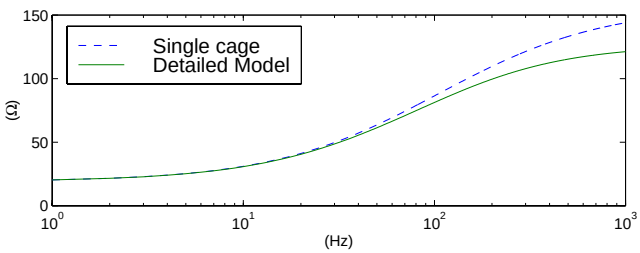

Fig. 5. Operational Impedance for the induction motor

The main reason behind the first detailed rotor models were to correctly assess the machine behaviour during transients such as startup, load change. In drive system even in steady state the converter will inject harmonic currents, each of them producing a distinct current distribution in the rotor bars. This implies in torque harmonics produced by the motor. The operational impedance of the motor can be used to evaluate how the motor impedance changes with the frequency. It has the same value on each axis, and for the a two cages rotor winding, the motor operational impedance X(s) is defined as:

$$X(s) = X_d \frac{(1+sT^{''})(1+sT^{'})}{(1+sT_0^{''})(1+sT_0^{'})} \tag{11}$$

where X_d is the motor direct axis reactance, equal to the sum of the magnetizing reactance and the leakage reactance of the stator [1]. $T^{'}$ and $T_0^{'}$ are respectively the transient short and open circuit time constants, and $T^{''}$ and $T_0^{''}$ are respectively the subtransient short and open circuit time constants [15]citeadkins. The values of the time constant can be calculated via the circuit parameters [16]. For a case where there is only one cage naturally $T^{''}$ and $T_0^{''}$ are zero.

Fig. 5 shows the operational impedance for a 100HP ESP induction motor. From this figure one can understand why a single cage model should be avoided when a harmonic environment is considered in the analysis. For the case of the motor under study in this research, over-damped results would be achieved whether a single cage rotor is used.

Fig. 4 shows this current, simulated and experimental. Again one might see the over-damped results achieve with only one rotor circuit. The experimental result shows that the result with a detailed model is much closer to the reality.

This over-damped behaviour leads to a lower harmonic content in the torque than the actual. To further illustrate the importance of the rotor modelling, Fig. 6 shows the stator current in a drive system where the motor is modelled as either double cage with the coupling between rotor circuits or the conventional single cage. Unfortunately, as said in the first part of this paper, the system had unaccess part, thus experimental results for the stator current were not available but the current in the converter output was measured.

IV. Conclusion

One of the problems in the motor modelling is data acquisition. Once a reliable set is achieved a stable an accurate model can be done. The simulation must give a result as near as possible to the actual system, to do so the eddy current in the motor and the skin effect in the cable should be taken into account.

The double cage with rotor coupling is necessary whether the harmonic effects in the motor are to be correctly evaluated. The cable model must be accurate to correctly rep-

[1]for induction motors X_d is identical to X_q

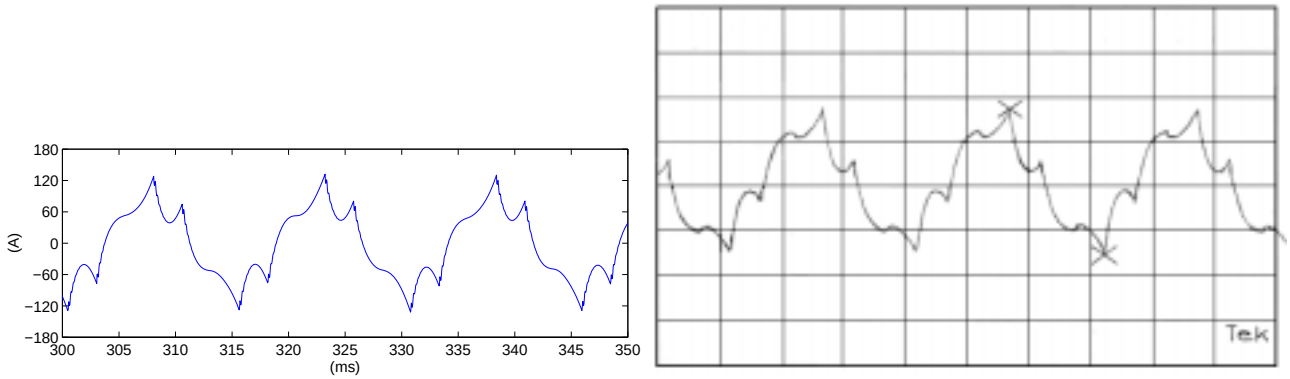

(a) Simulated

(b) Experimental (vert. 60A/div, hor. 2 ms/div)

Fig. 3. Cable Input Current – System with PAM-VSI

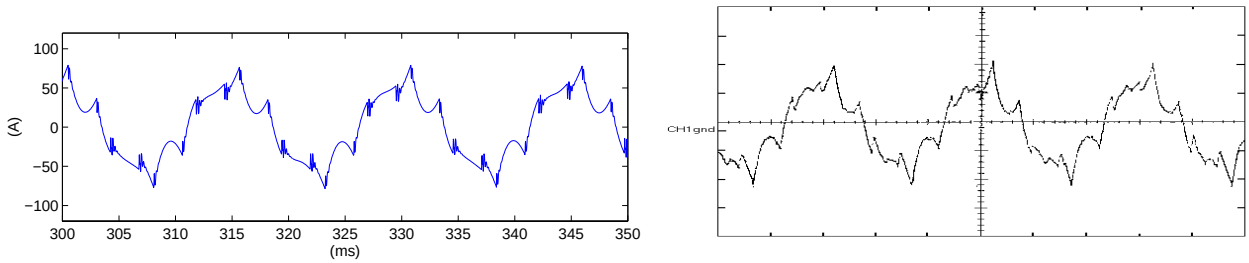

(a) Simulated

(b) Experimental (vert. 40A/div, hor. 5ms/div)

Fig. 4. Cable input current – System with PWM-VSI

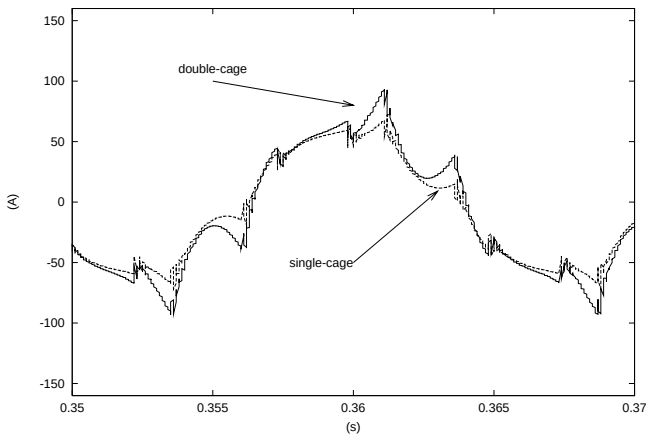

Fig. 6. Stator current for different rotor circuits

resent the voltage throughout the system and is discussed in an companion paper. The motor model is important to determine the output current as well as the torque developed by the motor. From the results of these two papers one can see that the cable model is necessary for a precise voltage calculation, while the motor with double cage is for a more correct current calculation.

Different converter performances are compared. The waveforms are generally far from sinusoidal, leading to a ripple in the electro-magnetic torque. This torque ripple is a very important issue, since ESP motors have very low inertia. This ripple can produce unexpected situations such as low order resonances in the motor shaft. The spikes in the voltages due to the switching can also be responsible for insulation failure in the motor windings.

Since the PWM converter is operating near a square wave mode, the currents are similar to the ones achieved with a PAM-VSI. The low frequency PWM is responsible for the switching the current as seen in Fig. 4.

Acknowledgment

The authors wish to express their gratitude to Mr.Jaime Mourente Miguel from PETROBRAS for providing the experimental results. Special thanks are also due to Prof.Hermann Dommel from the University of British Comlumbia for his kind comments and suggestions. This works was made possible through a research scholarship from CNPq.

References

[1] R. Hung and H. Dommel, "Synchronous machine models for simulation of induction motor transients," *IEEE Trans. on Power*

Systems, vol. 11, pp. 833–838, May 1996.
[2] M. Kazmierkowski and H. Tunia, *Automatic Control of Converter-Fed Drives*. Elsevier, 1994.
[3] I. M. Canay, "Determination of model parameters of synchronous machines," *IEE Proceedings.*, vol. 130, pp. 86–94, 1983.
[4] D. S. Babb and J. E. Williams, "Circuit analysis method for determination of ac impedance of machine conductors," *AIEEE Transactions*, vol. 70, pp. 661–666, 1951.
[5] B. Chalmers and A. Williamson, *AC Machines – Electromagnetics and Design*. John Wiley and Sons, 1991.
[6] E. A. Kingshirn and H. Jordan, "Simulation of polyphase induction machines with deep rotor bars," *IEEE Trans. on PAS*, vol. PAS-89, no. 6, pp. 1038–1043, 1970.
[7] W. Levy *et al.*, "Improved models for the simulation of deep bar induction motors," *IEEE Trans. on Energy Conversion*, vol. 5, pp. 393–400, Jun 1990.
[8] V. Honsinger, "Induction motor operating from inverters," *IEEE IAS Anual meeting*, pp. 1062–1071, 1980.
[9] R. D. Donker, "Field-oriented controllers with rotor deep bar compensation circuits," *IEEE Trans. on Ind. Appl.*, vol. IA28, pp. 1062–1071, Set 1992.
[10] R. Healey, A. Smith, and S. Williamson, "A transient induction motor model including saturation and deep bar effect," *IEEE Trans. on Energy Conversion*, vol. 11, pp. 8–15, Mar 1996.
[11] G. J. Rogers and D. Shirmohammadi, "Induction machine modeling for the electromagnetic transients program," *IEEE Trans. on Energy Conversion*, vol. 2, pp. 622–628, Dec 1987.
[12] A. C. S. de Lima, "Análise do sistema de acionamento eletrônico usado para a prospecção de petróleo," tese de M.Sc., Universidade Federal do Rio de Janeiro, 1997.
[13] R. Hung, "Synchronous machine models for simulating induction motors transients," Master's thesis, University of British Columbia, 1995.
[14] M. Nave, "Considerations for application of electrical submersible pumps for underground coal mine dewatering," *IEEE Trans. on Ind. Appl.*, vol. 25, pp. 846–850, Sept. 1989.
[15] A. Fitzgerald, *Electric Machines*. McGraw Hill, 1990.
[16] P. Krause, *Analysis of Electrical Machinery*. McGraw Hill, 1990.